

Germanium Subcells for Multijunction GaInP/GaInAs/Ge Solar Cells

N. A. Kalyuzhnyy^a, A. S. Gudovskikh^b, V. V. Evstropov^a, V. M. Lantratov^a, S. A. Mintairov^a,
N. Kh. Timoshina^a, M. Z. Shvarts^a, and V. M. Andreev^{a, b}

^aIoffe Physical Technical Institute, Russian Academy of Sciences, Politekhnicheskaya ul. 26, St. Petersburg, 194021 Russia

^ae-mail: nickk@mail.ioffe.ru

^bSt. Petersburg Academic University Nanotechnology Research and Education Center,

Russian Academy of Sciences, St. Petersburg, 195220 Russia

Submitted June 7, 2010; accepted for publication June 22, 2010

Abstract—Photovoltaic converters based on n -GaInP/ n – p -Ge heterostructures grown by the OMVPE under different conditions of formation of the p – n junction are studied. The heterostructures are intended for use as narrow-gap subcells of the GaInP/GaInAs/Ge three-junction solar cells. It is shown that, in Ge p – n junctions, along with the diffusion mechanism, the tunneling mechanism of the current flow exists; therefore, the two-diode electrical equivalent circuit of the Ge p – n junction is used. The diode parameters are determined for both mechanisms from the analysis of both dark and “light” current–voltage dependences. It is shown that the elimination of the component of the tunneling current allows one to increase the efficiency of the Ge subcell by ~1% with conversion of nonconcentrated solar radiation. The influence of the tunneling current on the efficiency of the Ge-based devices can be in practice reduced to zero at photogenerated current density of ~1.5 A/cm² due to the use of the concentrated solar radiation.

DOI: 10.1134/S106378261011028X

1. INTRODUCTION

Starting with the introduction of Soviet spacecraft with solar batteries based on homojunction gallium arsenide solar cells (SCs) and, later, from the design of the AlGaAs/GaAs heterostructures [1, 2], III–V based SCs have been successfully used for power supply of artificial satellites, gradually forcing out other types of photovoltaic converters from this sector, first of all, due to the radiation stability of this class of semiconductor devices.

As a result of the development of OMVPE technology (Organic-Metallic Vapor Phase Epitaxy), monolithic multijunction solar cells (MJ SCs) were fabricated. In these cells, a conventional Ge semiconductor is used as a substrate and simultaneously as a narrow-gap subcell for a wide-gap GaInP/GaAs double-junction SC [3–6].

Despite the development of mechanically stacked MJ SCs [7] and existing tendencies of an increase in the number of the p – n junctions [8], the monolithic three-junction solar cells based in the GaInP/GaInAs/Ge structure are currently the most competitive and effective solution for power supply of spacecraft [9] and are acquiring an increasingly large application in terrestrial photovoltaic power installations.

Thus, we can state that there is a rebirth of interest in the study of the Ge p – n junction, first of all, in connection with its use in a narrow-gap MJ SC subcell.

Germanium is a suitable substrate material for the OMVPE of the III–V semiconductor crystals. It possesses chemical compatibility with the Al–Ga–In–P and Ga–In–As compounds and ensures the absence of phase transitions with growing components. Germanium has close values of the thermal expansion coefficient and lattice constant to those in GaAs.

From the point of view of operation in space, an increased mechanical strength of Ge is essential. This provides a decrease in the thickness of the structures and weight of the SCs, and an increase in the specific (per unit weight) power output of the highly efficient solar cells.

In addition, the Ge p – n junction involved into the process of the photoconversion in the MJ SC allows one to extend its photosensitivity to a wavelength of 1800 nm (the Ge band gap is 0.66 eV at room temperature).

Previously, the Ge p – n junctions were actively studied in order to fabricate rectifiers, transistors, photodiodes, etc. It was established that the mechanism of flowing of the forward current is diffusion (nonideality factor $A = 1$), which is caused by the recombination of electrons and holes thermally injected into the quasi-neutral p - and n -regions of the p – n junction (the Shockley diffusion component [10, 11]). The diffusion saturation current was ~ 10^{-6} A/cm² at room temperature [12]. The recombi-

nation component caused by the recombination of electrons and holes thermally injected into the space charge region of the $p-n$ junction was absent. However, an excess (in Esaki terminology [13]) component was observed. With the reverse bias, this component gave saturation current density in the range 10^{-4} – 10^{-3} A/cm² (see § 12.2 in [14], [12]). In this case, the proper mechanism of the excess current in the non-degenerate Ge $p-n$ junctions was neither studied nor discussed.

However, we showed that the role of the excess component can be essential for the SC under the conditions of converting the low-intensity (the concentration ratio of the solar radiation $X < 1$), nonconcentrated ($X \approx 1$), and slightly concentrated ($X < 30$) solar radiation. Slightly concentrated solar radiation is realized in photovoltaic modules with the linear lens concentrators [15].

The goal of this study was to investigate the $n\text{-GaInP}/n\text{-}p\text{-Ge}$ photovoltaic heterostructure, which is intended for use as the “bottom subcell” of the three-junction GaInP/GaInAs/Ge SC. This heterostructure consists of a Ge $p-n$ junction and an $n\text{-GaInP}$ wide-gap window also functioning as the phosphorus source for the diffusion doping of the $p\text{-Ge}$ substrate with donors during formation of the $p-n$ junction.

We fabricated test Ge-based photovoltaic converters (PVCs) and studied the spectral dependences of their internal quantum yield (Q_{int}), “dark” and load (under illumination) current–voltage ($I-V$) characteristics. It is shown that dark $I-V$ characteristics should be approximated by the two-exponential model taking into account both the diffusion and excess components of the current. It is established that the excess component has the same temperature dependences as the excess tunneling components in the $p-n$ heterojunctions [16] and Schottky barriers [17]. We used the two-exponential model to approximate the photovoltaic dependences of the open-circuit voltage (V_{oc}) and efficiency (η) on photogenerated current J_g proportional to the intensity of illumination. The influence of the excess current on the conversion efficiency of solar radiation by the Ge-based photoconverter and, correspondingly, by the MJ SC, is established.

Thus, it is shown that the tunneling mechanism of the current should be taken into account in the photovoltaic Ge $p-n$ junctions along with the diffusion mechanism. The influence of the former on the device efficiency is especially essential in the conversion mode of slightly concentrated, nonconcentrated, and low-intensity solar radiation. The necessity to use the two-diode electrical equivalent circuit for the description of the Ge $p-n$ junction is shown.

2. OBJECTS OF THE STUDY

To fabricate the $n\text{-GaInP}/n\text{-}p\text{-Ge}$ structures, we used MOC–hydride epitaxy. The structures were grown in a laboratory installation with a horizontal reactor under a reduced pressure of 100 mbar. The crystal growth was carried out on $p\text{-Ge:Ga}(100)$ substrates 50 mm in diameter misoriented by 6° in the [111] direction.

As the sources of elements of Group III, we used the metal–organic compounds trimethylgallium (TMGa) and trimethylindium (TMIn). Arsine (AsH₃) and phosphine (PH₃) were used as the sources of Group V elements. The source of the doping impurity to obtain the n -type conduction was monosilane (SiH₄).

The $p-n$ junction in the Ge substrate was formed due to the diffusion of P atoms from the growing GaInP nucleation layer also playing the role of a wide-gap window for the Ge $p-n$ junction. The thus-grown heterostructure completely reproduces the narrow-gap Ge subcell in MJ SC. The $n^{++}\text{-GaAs}$ contact layer was grown for subsequent fabrication of the test Ge-based PVCs.

The contact structure of the Ge-based PVC was formed by photolithography. The configuration of the contact structure was developed for SCs intended for use in photovoltaic modules with linear lens concentrators [15]. The front surface of the PVC was covered with a ZnS/MgF₂ bilayer antireflection coating.

Under the different conditions of the growth of the GaInP nucleation layer, two groups of structures were grown. Structures of group 1 had the same thickness of the GaInP wide-gap window but various times of exposure to the PH₃ flow (various times of the gas diffusion of P atoms). Structures of group 2 had the same gas diffusion but various thicknesses of the GaInP layers (various times of the solid-phase diffusion of P). The thickness of the wide-gap window varied in the range of 35–300 nm. The time of the gas diffusion (annealing) at a high partial pressure of PH₃ was 5–40 min. The conditions of formation and parameters of the heterostructures are listed in the table.

3. THE ANALYSIS OF THE EXPERIMENTAL RESULTS

3.1. Spectral Characteristics of the Photoresponse of the Ge-based PVCs

We measured the spectral dependences of the external quantum yield of the photoresponse (Q_{ext}) and reflectance (r) for the Ge-based test PVCs with the structures grown under various conditions of the gas and solid-phase diffusion. The comparison of the heterostructures (Fig. 1) was performed by the internal quantum yield $Q_{\text{int}} = Q_{\text{ext}}(1 - r)$ in order to eliminate the influence of the difference in reflectances.

The values of the internal quantum yield for heterostructures with various times of the gas diffusion

Conditions of formation of the $n\text{-GaInP}/n\text{-}p\text{-Ge}$ photovoltaic heterostructures in MOC–hydride epitaxy and parameters of the Ge-based PVCs at 300 K

PVC no.	Annealing time in PH_3 , min	Thickness of the GaInP window, nm	J_g , mA/cm ² (AM0, $X = 1$, Q_{ext})	J_g , mA/cm ² (AM0, $X = 1$, Q_{int})	J_{0d} , 10^{-6} A/cm ² ($E_d = 0.025$)	J_{0t} , 10^{-3} A/cm ² ($E_t = 0.17$)	R_s , $\Omega \text{ cm}^2$
1	—	35	52.07	57.68	5.2	1.4	0.014
2	—	100	51.06	56.77	2.9	1.1	0.013
3	10	100	50.57	55.29	2.4	3.3	0.013
4	40	100	49.83	55.42	4.4	0.5	0.010
5	—	300	50.00	53.25	6.8	1.0	0.014

(2, 3, 4) but with the same thickness of the wide-gap window almost coincide over the entire spectral range. For structures with various thicknesses of the wide-gap window (1, 2, 5), the value of Q_{int} is substantially different only in the absorption region of GaInP, i.e., the variation in the photogenerated current (see table) is mainly determined by the absorption of the short-wavelength photons in the wide-gap window; it is almost independent of the conditions of formation of the $p\text{-}n$ junction. We note that the short-wavelength spectral region is unimportant when one uses of the heterostructure as a subcell in the MJ SC since this region is used by the upper wide-gap subcells.

Thus, the internal quantum yield is almost independent of both the preepitaxial conditions of annealing of the Ge substrate in PH_3 and the time of the epitaxial growth of the wide-gap material. Consequently, the excess P concentration in Ge is formed from the

near-surface GaInP nucleation layer rather than from the gas phase and does not increase with the subsequent growth of the wide-gap window. The location of the $p\text{-}n$ junction is determined by the spread of the concentration profile during the further growth of the structure. For the studied samples with various thicknesses of the GaInP layer this difference in time is inessential; therefore, the parameters of the $p\text{-}n$ junctions (the junction depth and the diffusion length of the carriers) are similar.

The depth of the diffusion $p\text{-}n$ junction in Ge was determined using the secondary-ion mass spectrometry (SIMS). The doping profile was peaked (up to $\sim 10^{20} \text{ cm}^{-3}$) near the Ge/GaInP heterointerface, while the depth of the $p\text{-}n$ junction for all the studied PVCs was ~ 140 nm.

It was shown [18, 19] that the preepitaxial conditions (for example, annealing in PH_3) determine the reconstruction of the surface of the Ge substrate and, consequently, the growth quality of the entire crystalline structure grown on the Ge substrate. Analysis of the behavior of the spectral characteristics of the photoresponse allows us to draw the following conclusions concerning the formation of the Ge $p\text{-}n$ junctions during the MOC hydride epitaxy. First, due to the fact that the photovoltaic properties of the Ge $p\text{-}n$ junction are independent of the conditions of annealing in PH_3 , it is possible to vary the latter in a wide range, based only on the requirements of ensuring a favorable reconstruction of the Ge surface. Second, since the thickness of the wide-gap window also does not affect the internal quantum yield of the photoresponse of the heterostructures, it is possible to vary it depending on the requirements to the device parameters.

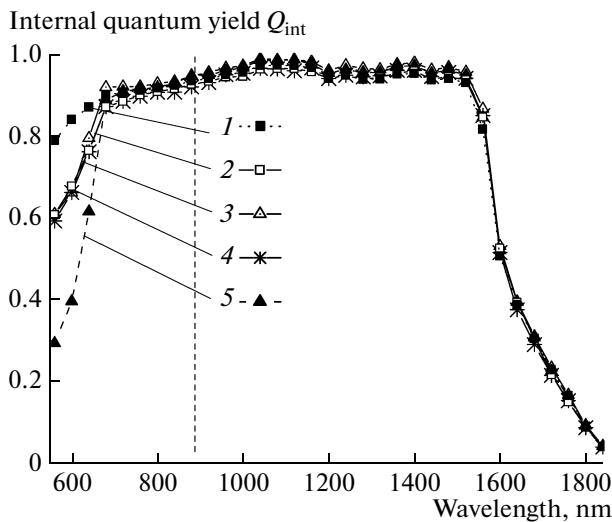


Fig. 1. Spectral dependences of the internal quantum yield of the photoresponse (Q_{int}) for the heterostructures obtained under various conditions of formation. Numbering of the curves corresponds to numbering of the samples in the table. The dashed vertical line separates the long-wavelength spectral region essential for the photovoltaic conversion of the Ge subcell in the composition of the MJ SC.

3.2. The Dark Current–Voltage Characteristics of the Ge $p\text{-}n$ Junctions

It is known that the main photovoltaic characteristics of the $p\text{-}n$ junction (for example, dependences of V_{oc} and efficiency on photogenerated current J_g) are determined from the dark $I\text{-}V$ characteristic; therefore, they are specified by the same parameters.

Figure 2 represents the dark forward and reverse I - V characteristics of the Ge-based PVC 4 (see table) measured in the temperature range of 77–300 K.

The approximation of the forward portion of the I - V characteristic by sum of exponential components (1a) showed that the forward current in the region of working temperatures (200–330 K) consists of the classical diffusion component and the excess component. It will be further shown that this component has a tunneling character:

$$J = J_{0d} \left[\exp\left(\frac{V - JR_s}{E_d}\right) - 1 \right] + J_{0t} \left[\exp\left(\frac{V - JR_s}{E_t}\right) - 1 \right], \quad (1a)$$

where J is the current density in the external circuit; V is the voltage; R_s is the series resistance of the device; J_{0d} is the saturation current (the preexponential factor) of the diffusion component; J_{0t} is the preexponential factor (saturation current) of the excess (tunneling) component; E_t is the characteristic potential of the tunneling component; and E_d is the characteristic (thermal) potential of the diffusion component, which can be expressed in terms of the nonideality factor $A_d = 1$ as

$$E_d = \frac{kT}{q} A_d = \frac{kT}{q}. \quad (1b)$$

Here, q is the elementary charge, k is the Boltzmann constant, and T is the absolute temperature.

Thus, the conventional in practice one-diode circuit (§ 3.9 in [20]) should be replaced by the two-diode circuit for the Ge p - n junction.

At 300 K, the saturation current density $J_{0d} \approx 10^{-6} \text{ A/cm}^2$, which agrees well with the Shockley data [12] for the Ge p - n junctions and corresponds to the diffusion mechanism of the current. The value of the reverse current extrapolated to the voltage zero (Fig. 2) coincides with the preexponential factor of the excess forward current J_{0t} ; it is close to the reverse currents observed previously by the order of magnitude ($\sim 10^{-4} \text{ A/cm}^2$) (see [12], § 12.2 in [14]).

The values of preexponentials (J_{0d}, J_{0t}) and characteristic potentials (E_d, E_t) for all the studied samples at 300 K are tabulated.

In the low-temperature region ($T < 120^\circ\text{C}$), the shape of the I - V characteristic (Fig. 2, curve 3) is apparently affected by the series (possibly nonlinear) resistance, which sharply (by an order of magnitude) increases as the temperature is decreased. In addition, the I - V characteristic at 100 K is approximated by the sum of only two excess components since the diffusion component, which decreases at a low temperature, does not manifest itself.

It is seen from the table that the presence of both the diffusion and excess current is the common property of all the studied p - n junctions and the character-

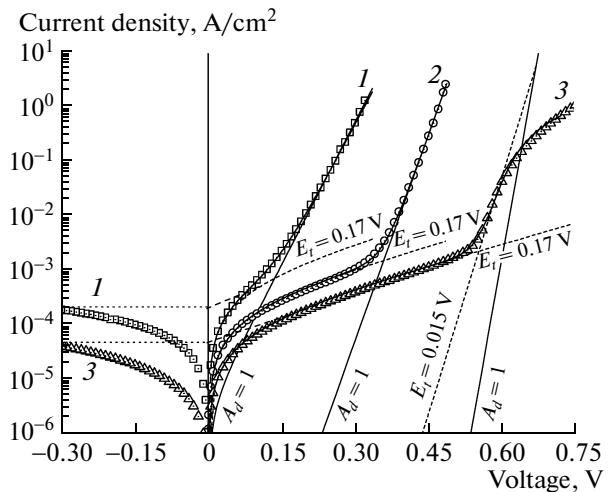


Fig. 2. Forward and reverse dark current–voltage characteristics of the Ge p - n junction at various temperatures: (1) 300 K ($J_{0d} = 4.4 \times 10^{-6} \text{ A/cm}^2$, $J_{0t} = 5 \times 10^{-4} \text{ A/cm}^2$), (2) 200 K ($J_{0d} = 1.4 \times 10^{-12} \text{ A/cm}^2$, $J_{0t} = 2 \times 10^{-4} \text{ A/cm}^2$), and (3) 100 K ($J_{0d} = 1.6 \times 10^{-34} \text{ A/cm}^2$, $J_{0t} = 9 \times 10^{-5} \text{ A/cm}^2$, $J_{0t} = 2.1 \times 10^{-19} \text{ A/cm}^2$). The points correspond to the experimental data; the thick solid lines correspond to the calculation by the two-exponential model; the thin solid lines correspond to the diffusion ($A_d = 1$) component of the forward current; the dashed lines correspond to tunneling components of the forward current, namely, the main ($E_t = 0.17 \text{ V}$) and additional ($E_t = 0.015 \text{ V}$); and the dotted lines correspond to the extrapolation of the reverse current to the zero voltage.

istic parameters (J_{0i} , E_i , where $i = d, t$) for both mechanisms of the current in different samples have values close to each other. This allows us to state that the presence of the diffusion and excess current is the typical situation for the Ge p - n junctions.

Figure 3 represents the temperature dependences of parameters J_{0i} and E_i obtained by approximation of the I - V characteristic by formula (1a) (see table, sample 4). To theoretically substantiate the nature of two mechanisms of the current in the Ge p - n junctions, the experimental temperature dependences of J_{0d} and J_{0t} are compared with calculated ones.

The relation for the diffusion saturation current J_{0d} can be written in a form with the temperature dependence of the band gap taken into account:

$$J_{0d} = q N_c N_v \left(\frac{D_{pN}}{n_N L_{pN}} + \frac{D_{nP}}{p_P L_{nP}} \right) e^{-E_g/kT}, \quad (2)$$

where N_c and N_v are the effective densities of states in the conduction band and in the valence band; D_{nN} , D_{pN} , and L_{nN} and L_{pN} are the diffusivities and diffusion lengths for the minority carriers in the P - and N -regions, respectively; n_N and p_P are the concentrations of the majority carriers in N -emitter and P -base; and E_g is the band gap.

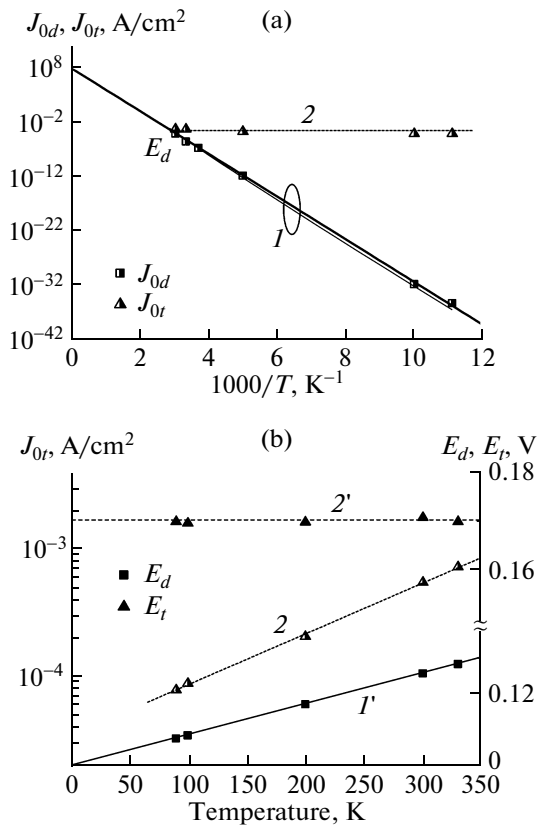


Fig. 3. Temperature dependences of the diode parameters in the (a) direct and (b) inverse temperature scales. (1) J_{0d} , (2) J_{0r} , (1') E_d , and (2') E_r . The points correspond to the experimental data, the dotted lines correspond to the approximation of the experimental dependences, and the solid lines correspond to the theoretical calculation. For curve I, the thick solid line corresponds to the calculation using formula (3) and the thin solid line corresponds to the calculation using formula (7).

The temperature dependence of E_g of Ge in a temperature range of 150–300 K is described by the well-known empirical formula (see § 10.1 in [14], § 2.17 in [20]):

$$E_g = E_{g0} - \beta T, \quad (3)$$

where the empirical constants $E_{g0} = 0.785$ eV and $\beta \approx 4.0 \times 10^{-4}$ eV/K.

In this case, formula (2) can be written as

$$J_{0d} = J_0^\infty e^{-E_a/kT}, \quad (4)$$

where activation energy $E_a = E_{g0}$, while J_0^∞ is a function of temperature that is weak compared with the exponential one. The approximation of the experimental data for J_{0d} by formula (4) at the mentioned value of E_a (Fig. 3a, thick solid line) allows us to obtain the experimental value $J_0^\infty \approx 1 \times 10^8$ A/cm² by the extrapolation to $T \rightarrow \infty$.

The calculated value of J_0^∞ at $T \rightarrow \infty$ in the exponent of formula (4) is described by the expression

$$J_0^\infty = q N_c N_v \left(\frac{D_{pN}}{n_N L_{pN}} + \frac{D_{nP}}{p_P L_{nP}} \right) e^{\beta/k}. \quad (5)$$

In this case, the estimate of the diffusivities is taken from the tabulated data for mobilities of electrons and holes in Ge [20, 21]; these quantities are $D_{nP} \leq 100$ and $D_{pN} \leq 50$ cm²/s. The diffusion lengths were established previously in [22] when analyzing the spectral characteristics of the Ge-based PVC and were $L_{nP} = 50$ and $L_{pN} = 0.35$ μm. The values of N_c and N_v for Ge, which are also temperature-dependent, are calculated using the expressions (see § 10.1 in [14])

$$N_c = 2 \times 10^{15} T^{3/2}, \quad N_v = 1.17 \times 10^{15} T^{3/2} \quad (6)$$

at temperatures for which empirical relation (3) is fulfilled.

As a result, the calculated value of quantity J_0^∞ varied from $\sim 8.7 \times 10^7$ A/cm² at $T = 300$ K to 1.4×10^8 A/cm² at $T = 350$ K, which agrees well with its experimental value.

Thus, the experimental values of the saturation current obtained at various temperatures (77–330 K) correspond to the diffusion mechanism of the current across the Ge *p*–*n* junction.

The use of the more exact (linear–quadratic) temperature dependence of E_g by the Varshni formula yields the same result [23]:

$$E_g = 0.742 - \frac{4.8 \times 10^{-4} T^2}{T + 235}. \quad (7)$$

The calculated dependence obtained by formula (2) with (7) taken into account approximates well the experimental values of preexponential factor J_{0d} over the entire temperature range under study (Fig. 3a, the thin solid line).

Characteristic potential E_d (Fig. 3b) is directly proportional to the temperature with nonideality factor $A_d = 1$ in (1b), which also confirms the diffusion nature of this component of the current.

Characteristic potential E_t for the component of the excess current is almost independent of temperature over the entire temperature range under study (Fig. 3b). In addition, preexponential factor J_{0r} is weakly temperature-dependent compared with the diffusion saturation current (Figs. 3a, 3b). These facts allow us to assume that the excess mechanism of the current has a tunneling nature. However, it is noteworthy that the tunneling-mechanism model is developed in insufficient detail compared with the diffusion model. This is, first of all, associated with the fact that the nature of the tunneling mechanism is rather complicated and involves the entire complex of transport phenomena of the charge carriers. Despite this fact, we evaluated temperature coefficient J_{0r} on the basis of the assumption of the tunneling nature of the excess component of the current.

According to the tunneling mechanism models [16, 24], the temperature dependence of preexponential factor J_{0t} should be determined by the temperature dependence of E_g ; therefore, it should be slightly ascending with an increase in temperature. The analysis of the experimental data showed an insignificant increase in J_{0t} upon increasing the temperature, which is described by the linear dependence (see Fig. 3).

If we assume that only the carriers located at the edges of the allowed bands participate in tunneling across the $p-n$ junction, i.e., disregard the thermal addition of the carriers in the bands, the tunneling current is written as [16]:

$$J_t = J_{0t} e^{V/E_t} = J_{00t} e^{(V-V_c)/E_t}, \quad (8)$$

where V_c is the contact potential difference between the quasi-neutral p - and n -regions. For a nondegenerate semiconductor, the value of qV_c is determined as the algebraic sum of the band gap of the semiconductor and chemical potentials for holes and electrons in the quasi-neutral regions:

$$qV_c = E_g - kT \ln\left(\frac{N_c}{n_N}\right) - kT \ln\left(\frac{N_v}{p_p}\right). \quad (9)$$

Substituting (9) into (8) and taking into account (3) and (6), we obtain the relation for the temperature coefficient:

$$b = \frac{\Delta \ln J_{0t}}{\Delta T} = \frac{1}{qE_t} \left[\beta + k \ln\left(\frac{N_c N_v}{n_N p_p}\right) \right]. \quad (10)$$

Temperature coefficient b calculated with formula (10) is $3 \times 10^{-3} \text{ K}^{-1}$ and coincides in order of magnitude with the value of $9.2 \times 10^{-3} \text{ K}^{-1}$ determined experimentally (Fig. 3b). The threefold excess of the calculated value over the experimental one is explained by the fact that formula (8) does not take into account the thermal-tunneling character of the current, which was previously analyzed only for the Schottky barriers [17].

The value of temperature coefficient b for preexponential factor J_{0t} , as well as the fact that the characteristic potential E_t is temperature-independent (Fig. 3b) is indicative of the tunneling nature of the excess component of the forward current.

Thus, the analysis of the dark $I-V$ characteristics and theoretical estimates obtained for the Ge $p-n$ junctions grown under various conditions allowed us to establish the presence of both the diffusion and tunneling components of the dark current, as well as to determine their parameters.

3.3. The Photovoltaic Characteristics of the Ge-Based PVC

We analyzed the family of the “light” $I-V$ characteristics (Fig. 4) measured at various concentration ratios of the solar radiation and approximated them

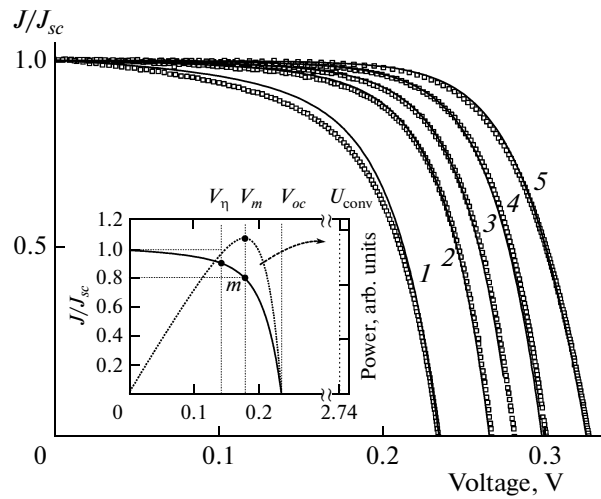


Fig. 4. Load portions of the “light” $I-V$ characteristics at various concentration ratios of the solar radiation $X = (1) 1, (2) 3, (3) 5, (4) 10$, and (5) 30. The curves are normalized to the corresponding values of the short-circuit current. The mutual arrangement of the voltages characterizing the shape of the $I-V$ characteristics, V_m , V_{oc} , V_η , as well as quantity U_{conv} are shown in the inset.

(the solid lines) using the suggested two-exponential model (1a), (1b) with the parameters presented in the table. In the range of concentration ratios of the solar radiation ($X < 30$) under consideration, series resistance R_s exerts no effect on the shape of the $I-V$ characteristics. All the load $I-V$ characteristics are normalized to the short-circuit current (J_{sc}), which in practice equals the photogenerated current ($J_{sc} \approx J_g$). The mentioned approximate equality is true since necessary condition $R_s \ll V_{oc}/J_{sc}$ is satisfied up to $J_{sc} \approx 50 \text{ A/cm}^2$.

For the load $I-V$ characteristic, the typical voltages convenient for description of its shape are usually used (Fig. 4, inset): V_{oc} , V_m , V_η . Here, V_{oc} is the voltage corresponding to the break of the external circuit; V_m is the voltage at the point (m) of the optimal load, in which its product by current J_m yields the maximal power (P_m) emitted on a load; and V_η is the “efficiency” voltage, which is determined by the equality

$$P_m = V_m J_m = V_\eta J_g. \quad (11)$$

Since the photogenerated current density is proportional to the power density of incident radiation P_{inc} , we can introduce auxiliary quantity U_{conv} , which is identical for all the load $I-V$ characteristics:

$$U_{conv} = \frac{P_{inc}}{J_g}. \quad (12)$$

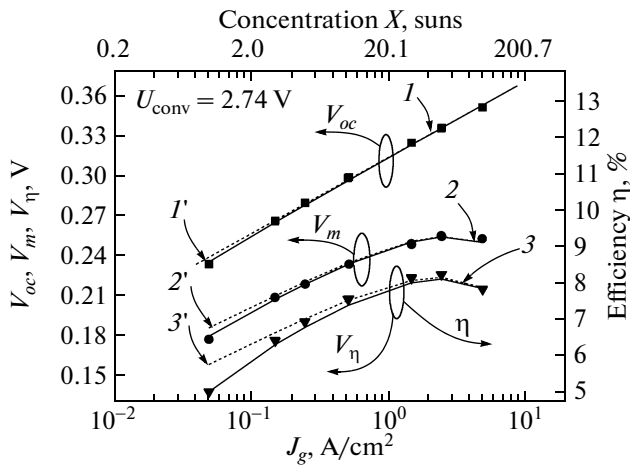


Fig. 5. Dependences of (1, 1') V_{oc} , (2, 2') V_m , and (3, 3') $V_\eta \propto \eta$ on the density of photogenerated current J_g . Curves (1, 2, 3) correspond to the experiment (the points) and to the approximation by the two-exponential model (the solid lines); curves (1', 2', 3') correspond to the approximation by the conventional single-exponential diffusion model (the dashed lines).

Thus, the efficiency voltage is directly proportional to the efficiency with coefficient U_{conv} :

$$\eta = \frac{P_m}{P_{\text{inc}}} = \frac{1}{U_{\text{conv}}} V_\eta. \quad (13)$$

Based on two-exponential model of the dark current (1a), (1b), we approximated dependences of V_{oc} , V_m , and V_η on photogenerated current J_g (Fig. 5). They consist of two components, namely, the diffusion and tunneling components, which are described by the same set of the diode parameters as the dark $I-V$ characteristic (see table). In other words, the approximation parameters (J_{0i} , E_i) can be found from analysis of the photovoltaic dependences only.

Dependence $V_{oc}(J_g)$ repeats the form of the nonresistive dark $I-V$ characteristic and can be approximated using relation (1a), where $R_s \rightarrow 0$ (in this case, $J \rightarrow J_g$, $V \rightarrow V_{oc}$). Therefore, dependence $V_{oc}(J_g)$ is most convenient for determining the parameters of the diffusion mechanism of the current. The thus-obtained values of preexponential factor J_{0d} and characteristic potential E_d of the diffusion component completely coincided with the values obtained from the analysis of the dark $I-V$ characteristic at 300 K.

To determine the parameters of the tunneling current, dependences $V_m(J_g)$ and especially $V_\eta(J_g)$ are most convenient since at any value of the photogenerated current, the contribution of the tunnel component to the “efficiency” voltage is largest compared with other characteristic voltages (Fig. 5). Thus, the preexponential factor of the tunneling current J_{0t} was refined using the numerical approximation of depen-

dences $V_\eta(J_g)$ and $V_m(J_g)$ by formulas obtained in [25] but allowing for the two-exponential model:

$$J_g = \sum_{i=d,t} J_{0i} [1 + \xi_i(V_\eta + J_g R_s)] \times \exp[\xi_i(V_\eta + J_g R_s)], \quad (14a)$$

where

$$\xi_i(V_\eta + J_g R_s) = \frac{V_{\eta 0} + \sqrt{V_{\eta 0}(V_{\eta 0} + 4E_i)}}{2E_i}, \quad (14b)$$

$$V_{\eta 0} = V_\eta + J_g R_s, \quad (14c)$$

and

$$J_g = \sum_{i=d,t} J_{0i} \left(1 + \frac{V_{m0}}{E_i}\right) \exp\left(\frac{V_{m0}}{E_i}\right), \quad (15a)$$

where

$$V_{m0} = V_m + J_g R_s. \quad (15b)$$

The shape of dependences $V_\eta(J_g)$ and $V_m(J_g)$ is affected by series resistance R_s . It decreases the characteristic voltages as the photogenerated current increases and leads to the emergence of a maximum. The calculated values of R_s are presented in the table.

It is evident that an increase in the tunneling current noticeably decreases the values of V_{oc} , V_m , and especially V_η at $X \leq 1$, and continues to affect the conversion efficiency of the solar radiation right up to $X \approx 30$. The elimination of the tunneling component of the current provides an increase in efficiency of the Ge-based PVC by up to 1% with the conversion of the nonconcentrated solar radiation with the AM0 spectrum (Fig. 5).

3.4. The Ge Subcell of the Multijunction Solar Cell

The Ge-based test PVCs considered above have the heterostructure similar to the narrow-gap MJ SC subcell. This fact allows us to evaluate the contribution of the Ge subcell to the photovoltaic characteristics of the MJ SC.

In this case, we should take into account the following features. The studied Ge-based PVCs have (see table) large values of the photogenerated current density ($J_g = J_{sc} = 49.8\text{--}52.1 \text{ mA/cm}^2$, $X = 1$, AM0). In the MJ SC, which is the series connection of subcells, the resulting short-circuit current is limited by the minimal of the currents generated by each $p-n$ junction, while the resulting voltage is the sum of subcell voltages. For the GaInP/Ga(In)As wide-gap tandem, the photogenerated current is highest when the magnitudes of J_{sc} of the upper (GaInP) and medium (GaInAs) subcells are matched (equal) at a maximally possible level [26]. Thus, the contribution of the Ge subcell to the efficiency of the MJ SC is limited by the resulting current of the upper wide-gap tandem; it is

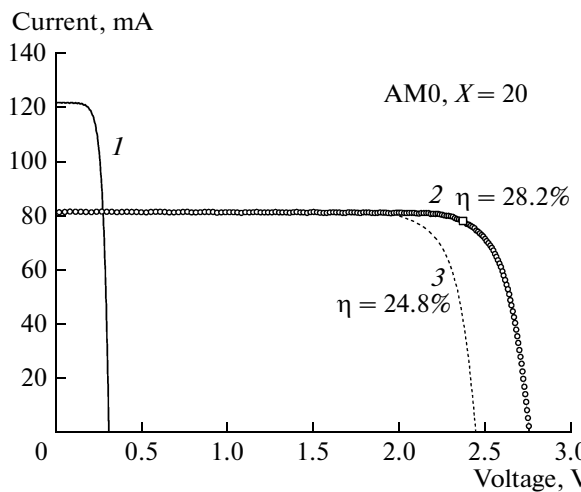


Fig. 6. Load current–voltage characteristics: (1) calculation by the two-exponential model (1) for the Ge subcell, (2) the experimental I – V characteristic for the GaInP/GaInAs/Ge three-junction SC, and (3) I – V characteristic simulated during the subtraction of 1 and 2 for the GaInP/GaInAs dual-junction SC.

determined by the magnitudes of V_{oc} and filling factor of the I – V characteristic (FF).

Nevertheless, an excess of the photogenerated current of the Ge subcell over J_{sc} of the wide-gap tandem is important, since the influence of the value of FF in the Ge subcell on the shape of the I – V characteristic of the MJ SC is minimal in this case.

In the MJ SC, the photogenerated current of the Ge subcell is lower than J_{sc} (see table) for the single Ge-based PVCs. Indeed, the GaInP/GaInAs wide-gap tandem serves as the optical filter for the Ge subcell and limits the range of its spectral photoresponse in the short-wavelength region because of the absorption of the radiation with wavelengths <890 nm in the GaInAs layers as shown by a vertical dotted line in Fig. 1.

Allowing for the mentioned features, we suggested the procedure for evaluating the contribution of the Ge subcell to the efficiency of the MJ SC. The MJ SCs were fabricated based on the GaInP/GaInAs/Ge monolithic three-junction structure grown by the OMVPE and had the design of contacts similar to the Ge-based test PVCs. The efficiency of the MJ SC was 26% with conversion of direct ($X = 1$) solar radiation and 28.2% with conversion of concentrated ($X = 20$) solar radiation (AM0).

The photogenerated current calculated for the GaInP/GaInAs optical filter was additionally corrected allowing for the difference in the properties of the antireflection coating of the Ge-based PVC and MJ SC. The value of J_{sc} obtained from the calculation was ~ 30 A/cm 2 , which noticeably exceeds J_{sc} for the wide-gap tandem.

Figure 6 shows the calculated load I – V characteristic of the Ge subcell (curve 1) and measured I – V characteristic of the MJ SC (curve 2) at $X = 20$. Subtraction of the voltages in curve 1 from voltages in curve 2 (Fig. 6) at fixed values of the current allows us to form the load characteristic of the GaInP/GaInAs wide-gap tandem (Fig. 6, curve 3) and calculate both its contribution and the contribution of the Ge subcell to the MJ SC efficiency. The efficiency of the Ge subcell in the composition of the GaInP/GaInAs/Ge three-junction SC was $\sim 2.3\%$ (AM0, $X = 1$). The contribution of the Ge subcell to the MJ SC efficiency increases as the multiplicity of the concentrating the solar radiation increases attaining $\sim 3.4\%$ at $X = 20$.

4. CONCLUSIONS

The n -GaInP/ n - p -Ge photovoltaic heterostructures intended for the use as the narrow-gap subcells of the GaInP/GaInAs/Ge three-junction solar cells for spacecraft are studied. It is shown that the maximal contribution of the Ge subcell to the conversion efficiency of the solar radiation by MJ SC (with $\eta = 28.2\%$, $X = 20$, AM0) can be as high as $\sim 3.4\%$.

It is for the first time shown (from the temperature dependences of the dark I – V characteristics in the range 77–330 K) that the excess current (along with the diffusion current) in the Ge photovoltaic p – n junctions has a tunneling character. As a result, to approximate the current–voltage (“dark” and “light”) characteristics and photovoltaic dependences (V_{oc} , V_m , and $V_\eta(\propto \eta)$ on $J_g(\propto X)$), it is necessary to use the two-exponential model taking into account both the diffusion and tunneling mechanisms of the current and the corresponding two-diode equivalent electrical circuit. The diode parameters are determined for both mechanisms of the current (J_{0d} , E_d , J_{0t} , E_t). It is shown that it is possible to determine all the diode parameters from both dark I – V characteristics and from the photovoltaic dependences only.

The influence of the tunneling current on the efficiency of the Ge subcell is evaluated. It is especially essential for low-intensity and nonconcentrated ($X \leq 1$) solar radiation, because of which a decrease in the efficiency of the Ge subcell with conversion of direct ($X = 1$) space solar radiation is $\sim 1\%$. The influence of the tunneling current in practice terminates upon increasing the concentration multiplicity up to $X \approx 30$ ($J_g \approx 1.5$ A/cm 2).

ACKNOWLEDGMENTS

We thank A.A. Usikova for preparation of the samples by photolithography and B.Ya. Ber, A.P. Koval'skii, and D.Yu. Kazantsev for the SIMS measurements.

This study was supported by the Russian Foundation for Basic Research, projects nos. 08-0800916-a and 09-08-12202-ofi_m.

REFERENCES

1. Zh. I. Alferov, V. M. Andreev, and V. D. Rumyantsev, *Fiz. Tekh. Poluprovodn.* **38**, 937 (2004) [Semiconductors **38**, 899 (2004)].
2. Zh. I. Alferov, V. M. Andreev, M. B. Kagan, I. I. Protasov, and V. G. Trofim, *Fiz. Tekh. Poluprovodn.* **4**, 1826 (1970) [Sov. Phys. Semicond. **4**, 785 (1970)].
3. J. M. Olson, S. R. Kurtz, A. E. Kibbler, and P. Faine, in *Proc. of the 21st IEEE PVSC* (Kissimmee, 1990), vol. 1, p. 24.
4. P. K. Chiang, D. D. Krut, B. T. Cavicchi, K. A. Bertness, S. R. Kurtz, and J. M. Olson, in *Proc. of the 1st World Conf. on Photovoltaic Energy Conv.* (1994), p. 2120.
5. P. K. Chiang, J. H. Ermer, W. T. Nishikawa, D. D. Krut, D. E. Joslin, J. W. Eldredge, B. T. Cavicchi, and J. M. Olson, in *Proc. of the 25th IEEE PVSC* (Washington, D.C., 1996), p. 183.
6. R. R. King, N. H. Karam, J. H. Ermer, M. Haddad, P. Colter, T. Isshiki, H. Yoon, H. L. Cotal, D. E. Joslin, D. D. Krut, R. Sudharsanan, K. Edmondson, B. T. Cavicchi, and D. R. Lillington, in *Proc. of the 28th IEEE PVSC* (Anchorage, 2000), p. 998.
7. M. Z. Shvarts, P. Y. Gazaryan, N. A. Kalyuzhnny, V. P. Khvostikov, V. M. Lantratov, S. A. Mintairov, S. V. Sorokina, and N. Kh. Timoshina, in *Proc. of the 21st EPSEC* (Dresden, Germany, 2006), p. 133.
8. D. C. Law, D. Bhusari, S. Mesropian, J. C. Boisvert, W. D. Hong, A. Boca, D. C. Larrabee, C. M. Fetzer, R. R. King, and N. H. Karam, in *Proc. of the 34th IEEE PVSC* (Philadelphia, PA, 2009).
9. M. Stan, D. Aiken, B. Cho, A. Cornfeld, J. Diaz, A. Korostyshevsky, V. Ley, P. Patel, P. Sharps, and T. Varghese, in *Proc. of the PVSC'08, 33rd IEEE* (2008), p. 1.
10. W. Shockley, *Bell System Tech. J.* **28**, 435 (1949).
11. S. M. Sze, *Physics of Semiconductor Devices* (Wiley, 1981; Mir, Moscow, 1984), ch. 14.2.
12. F. S. Goucher, G. L. Pearson, M. Sparks, G. K. Teal, and W. Shockley, *Phys. Rev.* **81**, 637 (1951).
13. *Tunneling Phenomena in Solids*, Ed. by E. Burstein and S. Lundqvist (Plenum, New York, 1969; Mir, Moscow, 1973), ch. 5.
14. R. A. Smith, *Semiconductors* (Cambridge Univ., Cambridge, 1959; Inostr. Liter., Moscow, 1962).
15. M. Z. Shvarts, O. I. Chosta, V. A. Grilikhes, V. D. Rumyantsev, A. A. Soluyanov, J. Vanbegin, G. Smekens, and V. M. Andreev, in *Proc. of the 31th IEEE PVSC* (Lake Buena Vista, FL, 2005), p. 818.
16. B. L. Sharma and R. K. Purohit, *Semiconductor Heterojunctions* (Pergamon, Oxford, 1974; Sov. Radio, Moscow, 1979), ch. 1. 1.
17. R. Stratton, in *Tunneling Phenomena in Solids*, Ed. by E. Burstein and S. Lundqvist (Plenum, New York, 1969; Mir, Moscow, 1973), ch. 8.
18. N. A. Kalyuzhnny, V. M. Lantratov, S. A. Mintairov, M. A. Mintairov, M. Z. Shvarts, N. Kh. Timoshina, and V. M. Andreev, in *Proc. of the 23th EPSEC* (Valencia, 2008), p. 803.
19. N. A. Kalyuzhnny, S. A. Mintairov, M. A. Mintairov, and V. M. Lantratov, in *Proc. of the 24th EPSEC* (Hamburg, Germany, 2009), p. 538.
20. R. P. Nanavati, *An Introduction to Semiconductor Electronics* (McGraw-Hill, New York, 1963; Svyaz', Moscow, 1965).
21. J. I. Pankove, *Optical Processes in Semiconductors* (Prentice-Hall, Englewood Cliffs, NJ, 1971; Mir, Moscow, 1973), appl. 2.
22. S. A. Mintairov, V. M. Andreev, V. M. Emel'yanov, N. A. Kalyuzhnny, N. K. Timoshina, M. Z. Shvarts, and V. M. Lantratov, *Fiz. Tekh. Poluprovodn.* **44**, 1118 (2010).
23. Y. P. Varshni, *Physica* **34**, 149 (1967).
24. A. G. Milnes and D. L. Feucht, *Heterojunctions and Metal-Semiconductor Junctions* (Wiley, New York, London, 1972; Mir, Moscow, 1975), ch. 2.
25. V. M. Andreev, V. V. Evstropov, V. S. Kalinovskii, V. M. Lantratov, and V. P. Khvostikov, *Fiz. Tekh. Poluprovodn.* **43**, 671 (2009) [Semiconductors **43**, 644 (2009)].
26. V. M. Lantratov, N. A. Kalyuzhnny, S. A. Mintairov, N. Kh. Timoshina, M. Z. Shvarts, and V. M. Andreev, *Fiz. Tekh. Poluprovodn.* **41**, 751 (2007) [Semiconductors **41**, 727 (2007)].

Translated by N. Korovin